Research Statement

Yen-Hsi Richard Tsai

October 2001

Since the introduction of the level set method [46] [51] for interface evolution, Hamilton-Jacobi equations which are homogeneous of degree one in the gradient of the solution have become a very important topic in both theoretical and numerical analysis of PDEs; e.g. [16, 22, 33] and [15, 35, 52, 55, 61]. One can find a wide range of different fields involving this type of equation; e.g. optimal control, etching, computer graphics and vision [48].

This article documents work that ranges from the basic step of level set methods, that is, constructing level set functions, to extending the level set method to more general equations and applications. For clarity, I will begin by giving a summary of my research, followed by a slightly more in-depth exposition of each of the four topics and a brief projection to the future research possibilities.

With Giga and Osher, I worked on extending and computing a generalization of the viscosity solution [16] to a wider class of Hamilton-Jacobi Equations, including conservation laws, whose solutions develop discontinuities in finite time. In [65], the graph of the solution is embedded as the zero level curve of a function satisfying the corresponding HJ equations in one dimension higher. A special singular diffusion is combined with the level set equation to keep the zero level curve as the graph of the solution at all time. We provide numerical methods for each type of the Hamiltonians considered, and our results show an agreement between the solution obtained this way with the entropy solution in the case of scalar conservation laws, and with the results predicted by Giga et al [28, 29].

In [47], we extended the level set method to applications such as ray tracing that need, in some sense, multi-valued solutions. Our approach is a classical yet novel one — instead of solving the equation in physical space, we solve the equivalent Liouville equation in the reduced phase space, thus avoid the difficulty of multi-valuedness. We use the vector level set technologies developed in [12, 53] to construct numerical approximations of the solution. Transmissions that satisfy Snell's Law can be computed directly using our numerical approach. Reflections are handled by solving a simple initial-boundary-value problem. A side project to this topic is to visualize the intersections of high dimensional zero level sets. Our current preliminary approach is to flow a set of points to the intersection through minimization.

Related to ray tracing, the visibility problem that occurs in many applications has also been studied. The problem is as follows: given an observer at x_o, and a collection of closed surfaces S, find the portions of S that are visible from x_o. We came up with a level set based multi-resolution algorithm that gives the the visible/invisible regions of the whole space. In addition, we gave a theoretical answer to the visibility problem at hand and derived the dynamics of the visible regions when the observer is moving.

A portion of my work is related to finding the "distance" function to given interfaces. The distance function is the viscosity solution of the eikonal equation subject to appropriate boundary conditions. It is a way to construct and reinitialize the level set function suitable for numerical operations. In [66], based on some geometrical consideration and Huygens' principle, a fast and accurate Gauss-Seidel type scheme is developed to find the distance to a set of isolated points and line segments. Also in the same article, a similar scheme utilizing the "closest surface element" map to provide close initial guess for Newton's iterations is developed to find the distance to smooth, explicitly defined, geometrical objects. In addition, in [67], a Godunov flux for the anisotropic quadratic

Hamiltonian is derived and coupled with the same iterative procedure to find the distance on graphs.

Contents

1 Computing discontinuous solution to a class of Hamilton-Jacobi Equations[1]

In 1983, Crandall and Lions [16] first introduced the notion of viscosity solution for this type of equations, based on a maximum principle and the order preserving property of parabolic equations. In general, for any given Hamilton-Jacobi equation of the form

$$u_t + H(x, t, u, Du) = 0,$$

where H is a continuous function from $\Omega \times \mathbb{R}^+ \times \mathbb{R} \times \mathbb{R}^n$, non-decreasing in u, and Ω is an open subset of $\mathbb{R}^n$, there exists a unique uniformly continuous viscosity solution if the initial data is bounded, uniformly continuous.[2] The continuity of the solution can be understood intuitively from the 1D fact that "HJ equations are the conservation laws integrated once." The viscosity solution is sometimes understood as the limit of the solutions to the equation with vanishing viscosity.

Correspondingly, Crandall and Lions in [15] proved the convergence of two approximations to the viscosity solution of equations whose Hamiltonians only depend on Du. This was generalized by Souganidis to equations with variable coefficients in [61]. Many sophisticated numerical methods have since been developed [35][42][51][52].

However, there are problems in control theory and differential games which demand discontinuous solutions. The original viscosity theory does not apply to discontinuous initial data. The notion of semi-continuous viscosity solution was first introduced by Ishii [32, 34]. Because of the non-uniqueness in Ishii's result, other notions of semi-continuous solutions were proposed by various authors [5][6] with different kinds of additional properties imposed on the Hamiltonian. Some of these notions need serious restrictions on the Hamiltonians and others are implicit in the sense that the processes of taking supremum and infimum are involved. As a consequence, one cannot develop numerical methods to construct approximations.

Finally, for the class of equations with Hamiltonians $H(x, u, Du)$ nondecreasing in u, the authors in [29] introduced a new notion for semi-continuous solution. This notion of solution is defined by the evolution of the zero level curve of the auxiliary level set equation which embeds the original HJ equation, an approach first described in [46]. It is thus called the L-solution. An immediate gain from this embedding is that we have a Lipschitz continuous Cauchy data for the level set Hamilton-Jacobi equation.

When the Hamiltonian $H(t, x, u, Du)$ is not nondecreasing in u, the solution may develop shocks in finite time even if the initial data is continuous. A new notion called the proper viscosity solution was introduced in [28] to track the whole evolution. This notion is consistent with the entropy solution when the equation is a conservation law. We extend the L-solution approach for this class of HJ equations with the introduction of a singular diffusive term in the vertical direction to the auxiliary level set equations so that the level curves will not overturn.

For the class of HJ equations nondecreasing in u, we applied a straightforward Lax-Friedrichs type scheme to the corresponding level set equations. This Lax-Friedrichs scheme is extended to higher order accuracy using the WENO approximation for the partial derivatives [52]. We showed numerically that the singular diffusion term can be applied to compute the shock solution for the more general class of HJ equations. In the case of conservation laws, the shock solutions we obtain from the regularized level set equations satisfy the "equal area" entropy condition and thus demonstrate the validity of our regularization terms. We emphasize, that based on our numerical results, the *global* property of our singular diffusion term regularizes our nonconservative level set equations such that the entropy condition is satisfied during the time iterations.

Lastly, we remark here that our numerical schemes for the derived level set equations can be computed locally around the zero level curve using the technique described in [53] for efficiency.

[1] Joint work with Y. Giga and S. Osher. To appear in Mathematics of Computation

[2] Notice that the conservation laws do not fall into this category because the corresponding H might not be monotone in u; e.g. shocks generally develop from smooth initial data.

Model Equations

We first consider the scalar 1D equation $u_t + H(x, u, u_x) = 0$ with the Hamiltonian satisfying the following properties: 1) H is Lipschitz in all its arguments; 2) $\lim_{\lambda \to 0} \lambda H(x, u, p/\lambda)$ exists. In addition, we are concerned with the following two classes of equations: 1)Equations with $H_u \geq 0$ but with discontinuous initial data; 2)Equations such as conservation laws that do not belong in the first class.

Let us consider the following two model equations, both of which can be in either the first or the second class depending on the parameters:

- Equations that contains both terms from conservation laws and fully nonlinear first order terms:

$$u_t + uu_x + a\, u|u_x| = 0,\ a \in \mathbb{R}; \tag{1}$$

  The associated level set equation reads

$$\phi_t - y \cdot (a\, \text{sign}(\phi_y)\, |\phi_x| - \phi_x) = 0. \tag{2}$$

- Equations that prescribe the normal motion of the graph of u:

$$u_t - v(u)\sqrt{1 + u_x^2} = 0; \tag{3}$$

  The corresponding level set equation is

$$\phi_t + \text{sign}(\phi_y)\, v(y)|\nabla \phi| = 0. \tag{4}$$

  The function v is the normal velocity of the graph of u, or the level sets of ϕ. If v ever decreases, then $H_u \leq 0$ and the equation fails to be in the first class.

Geometrical Explanation of the Non-overturning Conditions

We need to pay special attention in order to prevent the overturning of the level curves of ϕ. One equivalent criterion is to demand the minimum principle: $\phi_y(x, y, t) \geq 0$ for $t \geq 0$. If this criterion is met, we can ignore the term $\text{sign}(\phi_y)$ in the level set equation.

Minimization principle

The assumption that the Hamiltonian is non-decreasing in u has an important consequence. We present here an argument about this minimum principle based on an argument in [29]. Consider $\phi^h(x, y, t) := \phi(x, y + h, t)$, where $h > 0$ and $\phi(x, y, t)$ is the uniformly continuous viscosity solution of the level set equation $\phi_t + H(x, y, D\phi) = 0$ with uniformly continuous initial data $\phi_0(x, y)$. By a comparison principle [25][33], we proved that if $\phi^h(x, y, 0) - \phi(x, y, 0) \geq 0$ for all x and y, then $\phi^h(x, t) \geq \phi(x, t) \geq 0$!This basically says that if $\phi_y(x, y, t = 0) \geq 0$ initially, then $\phi_y(x, y, t) \geq 0$ for all time! It also implies that $\{\phi = c\}$ *will remain as a graph throughout the evolution.*

In addition, we also showed that with suitable CFL condition, our schemes keep the discrete version of this important property of this class of HJ equations.

Figure 1: Overturning is caused by the normal velocity which is increasing in the y-direction.

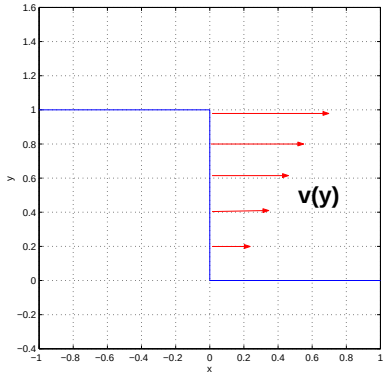

Figure 2: Example of concavification. Left: the concavification of the flux in Buckley-Leverett equation. Right:$V(y) = y^2/2$ on $[0, 1]$. The minimum value of M should be $1/8$.

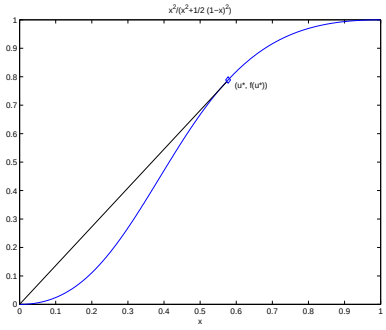

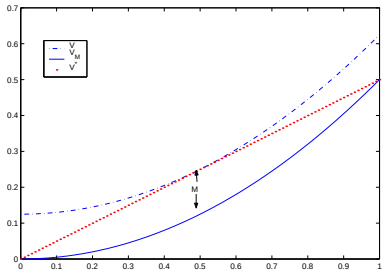

Convexification

In light of the level set equation (4), we have a more geometrical requirement on the speed function v. By the method of characteristics, we know that $v(y)$ prescribes the normal velocity of the level sets of ϕ. On the vertical segments of the level sets, which correspond to jumps in u, $v(y)$ prescribes the horizontal velocity according to y. Overturning will happen if $v(y)$ is increasing, since the upper part of the jump of u moves faster than the lower part. See figure 1.

Consider the primitive function of v:

$$V(y) = \int v(s)ds.$$

The non-increasing condition of v translates to the *concavity* of V! This fact reminds us of one of the entropy conditions for conservation laws with non-concave flux function. It says that the entropy solution of the conservation law with non-convex flux f is the classical solution of the conservation law with the flux f^*, where f^* is the minimal concavification of f over the increasing jump interval. This, in turn, provides us a hint on the regularization of HJ equations (4) — we need to impose a regularization that concavifies the primitive function on the vertical segments of the level sets and nowhere else. We have demonstrated numerically that our proposed singular diffusive regularization term does exactly [65]. See figures 3 and 4.

Figure 3: Numerical solutions of the Riemann problem for conservation laws obtained from our level set method. Left: Burgers' equation with multiple jumps. Right: Non-convex Buckley-Leverett Equation with flux $f(u) = u^2/(u^2 + 1/2(1-u)^2)$. The solution (green curve) obtained without singular diffusion is super-imposed to show the equal area rule.

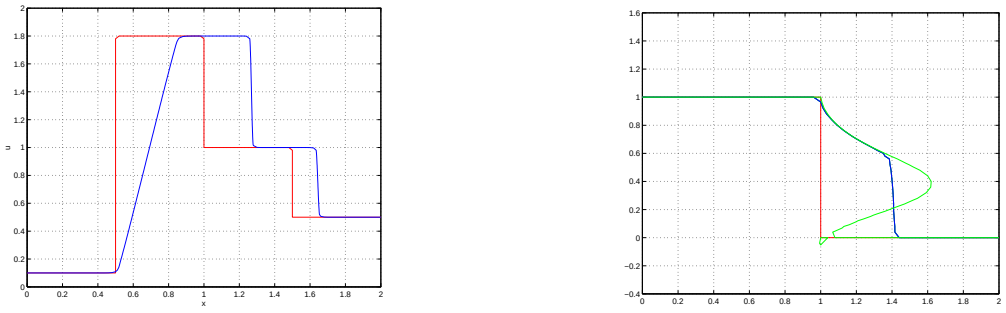

Figure 4: An example of a two dimensional calculation with (right) and without (left) vertical diffusion. The blue surface is the initial discontinuous data. The green and yellow surfaces are the solutions to $u_t - u\sqrt{1 + u_x^2 + u_y^2} = 0$ at different times.

Singular diffusion

Motivated by the work on a type of singular diffusion in [23, 24, 38], we will add a similar singular diffusion term in the y-direction to both our model equations:

$$M|\nabla\phi|\frac{\partial}{\partial y}(\frac{\phi_y}{|\phi_y|}).$$

We first notice that this viscosity is activated *only when* $\text{sign}(\phi_y) = \phi_y/|\phi_y|$ changes signs! With M sufficiently large, this term $\partial(\text{sign}(\phi_y))/\partial y$ can be shown, at least formally, to concavify the primitive of the speed function on the vertical part of the level sets [27].

We briefly describe how to find the minimum value of M. Consider the primitive function $V(y)$ of the speed function $v(y)$ of equation (3) over $[a, b]$ that is a jump of u. Let V^* be the function whose graph is the upper boundary of the convex hull of V. Let $V_M = V^* + M$. We claim that M has to be large enough such that V_M is tangent to or never crosses V^*. See figure 2 for an example with $V(y) = y^2/2$. Since the purpose of this paper is to provide the numerics, we refer the reader to the recent paper of the second author [27] for a formal reasoning.

Figure 3 and 4 show some examples of our computational results.

2 A phase space level set method and its application to geometrical optics[3]

Geometrical optics is an important area of study, especially as an approximation for high frequency wave propagation [37] in fields including electromagnetics, elastics, acoustics and seismology. Ray tracing, which uses a Lagrangian formulation to track quantities such as amplitudes and travel times along the wavefront by solutions of the related Hamiltonian system, is the de facto computational method. In the numerical implementation, wavefronts are represented by a finite set of particles, which are then evolved according to the Hamiltonian ODE system. This approach, though easy to understand, suffers from poor spatial resolution in an expanding wavefront.

Eulerian approaches solve the viscosity solution of the Hamilton-Jacobi PDEs of geometrical optics. The spatial resolution of the wavefront is simply controlled by the step size of the underlying grid. However, these approaches have difficulties when the wavefront becomes multivalued because the HJ equations are written for a single phase of the wavefronts at each point in space. Multiple phases occurs when rays cross or caustics appear, a phenomenon which is handled automatically when using Lagrangian methods.

There are several approaches to overcoming this difficulty. In [7, 8], the authors separate the domain of interest by caustics and compute different branches of the viscosity solutions in these regions and super-impose them in the end. Steinhoff et. al. [63] formulate the front propagation problem by DSE, a formulation which can be considered to be "orthogonal" to that using level sets. Ruuth et. al. made some improvements on the original work of [63] in [56]. However, this approach encounters difficulties involving interpolation and resolution as ray tracing does. The authors in [20] derived a system of conservation laws from the geometrical optics PDE to find multi-phase solution up to a predescribed number of phases. Recently, in [21], Engquist et. al. solve the wavefront propagation problem in phase space using the segment projection method [64] for wavefront representation in phase space.

We present a level set approach for following the representation of the wavefront in a reduced phase space. Under this representation, the reduced Liouville equations translate into a system of partial differential equations. Thus, altogether, we introduce here an Eulerian and PDE approach operating in reduced phase space for ray tracing and constructing wavefronts that handles multivalued solutions and spatial resolution of the wavefront automatically.

General formulation

Due to the constraint in space, we present our method in its most general form followed by details in the two dimensional case. We are given a Hamilton-Jacobi equation in $\mathbb{R}^n \times \mathbb{R}^+$ and its characteristic equations

$$\tilde{\phi}_t + H(\mathbf{x}, \nabla\tilde{\phi}) = 0, \quad \frac{d\mathbf{x}}{dt} = H_{\mathbf{p}}, \frac{d\mathbf{p}}{dt} = -H_{\mathbf{x}};$$

the corresponding Liouville equation is a linear PDE which shares *the same* characteristics equations:

$$u_t + H_{\mathbf{p}} \cdot \nabla_{\mathbf{x}} u - H_{\mathbf{x}} \cdot \nabla_{\mathbf{p}} u = 0. \tag{5}$$

For any time independent Hamiltonian homogeneous in $\nabla\tilde{\phi}$, (5) can be reduced by one if we set locally $\Theta = \mathbf{p}/|\mathbf{p}| \in S^{n-1}$ and write the partial derivatives $\nabla_{\mathbf{p}} u$ in terms of $\nabla_\Theta u$. The reduced phase space takes the form $\mathbb{R}^n \times S^{n-1}$, which has dimension $2n-1$, with bicharacteristic strips of dimension $n-1$. Thus the codimension of the bicharacteristic strips is n.

[3] Joint work with S. Osher, L.T. Chang, M. Kang, and H. Shim. Submitted to J. Comput. Phys.

Level set formulation

We follow the approaches used in [10] for a representation of wavefronts. We introduce the "vector" level set function $\Phi : \mathbb{R}^{2n-1} \times \mathbb{R}^+ \mapsto \mathbb{R}^n$ whose zeros of Φ represent the bicharacteristic strips at each fixed time. PDE's for the evolution of Φ can be derived from Liouville equation (5).

In the case of eikonal equation $\tilde{\phi}_t + c(x)|\nabla_x \tilde{\phi}| = 0$ in two dimensions, we solve

$$\Phi_t + v \cdot \vec{\nabla}\Phi = 0$$

where $v(x,\theta) = (c(x)\cos\theta, c(x)\sin\theta, c_{x_1}(x)\sin\theta - c_{x_2}(x)\cos\theta)'$. In the following subsections, unless otherwise noted, we consider only the two dimensional case.

Regularizing the level set functions

Let $\Phi = (\phi, \psi)'$. For numerical stability reasons, we maintain ϕ and ψ as signed distance functions around their zero level sets by solving to steady state

$$\tilde{\phi}_\tau + \text{sign}(\tilde{\phi}_0)(|\nabla\tilde{\phi}| - 1) = 0, \quad \tilde{\psi}_\tau + \text{sign}(\tilde{\psi}_0)(|\nabla\tilde{\psi}| - 1) = 0, \tag{6}$$

and in addition, we enforce the orthogonality of the zero level sets of ϕ and ψ by solving to steady state

$$\tilde{\phi}_\tau + \text{sign}\,(\tilde{\psi}_0)\frac{\nabla\tilde{\psi}}{|\nabla\tilde{\psi}|} \cdot \nabla\tilde{\phi} = 0, \quad \tilde{\psi}_\tau + \text{sign}\,(\tilde{\phi}_0)\frac{\nabla\tilde{\phi}}{|\nabla\tilde{\phi}|} \cdot \nabla\tilde{\psi} = 0; \tag{7}$$

where $\tilde{\phi}_0$ and $\tilde{\psi}_0$ are ϕ and ψ respectively, at that time step t, and τ is the artificial time.

Discretization

The PDEs mentioned above are discretized using fifth order WENO in space and third order TVD RK [52] or fourth order SSP RK of [62].

Reflection as an IBVP

Let $\partial\Omega$ denote the reflecting boundary with outward normal θ_n. Let θ_I and θ_R denote the angle of the incoming wavefront respectively on Ω. Then these two quantities obey the rule of reflection:

$$\theta_R = 2\theta_n - \theta_I + \pi,$$

where θ_R is taken in the branch $[-\pi, \pi]$. We evolve $\Psi : \mathbb{R}^2 \times S^1 \mapsto \mathbb{R}^2$ in Ω with the boundary conditions that on $\partial\Omega$,

$$\Psi(\theta) = \pm\Phi(2\theta_n - \theta + \pi)$$

and the initial condition[4]

$$\Psi_i|_\Omega = \mp\infty.$$

Here, we assume that initially $\Phi_i \geq 0$ at the boundary.

[4] In numerical calculations, we only need to choose a number larger then $||u_i||_\infty$.

Figure 5: The bicharacteristic strip in reduced phase space associated to the wavefront from an ellipse moving inwards. Note it is smooth and vertical above the nonsmooth points of the wavefront.

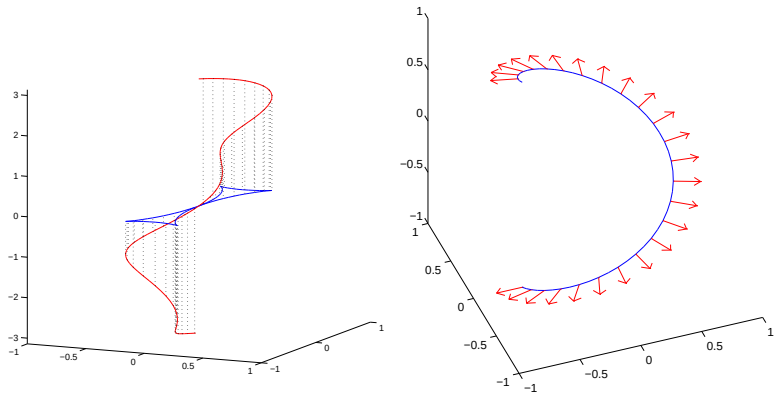

Intensity

For the constant index of refraction case, the intensity A^2 is a conserved quantity in time and changes only by geometrical spreading. It can be obtained from a passive calculation involving the Jacobian of the level set functions. In general, the intensity can be computed from the equation

$$A^2 = \int w d\mathbf{p},$$

where $w(\mathbf{x}, \mathbf{p}, t)$ is the density. As usual, we rewrite w in the reduced form and propagate by the same Liouville type PDE for the level set functions. Calculating the intensity is a simple passive operations, requiring the density to be propagated along with curve location.

Figure 6: A more detailed look at the evolution of the ellipse, plotted at different times.

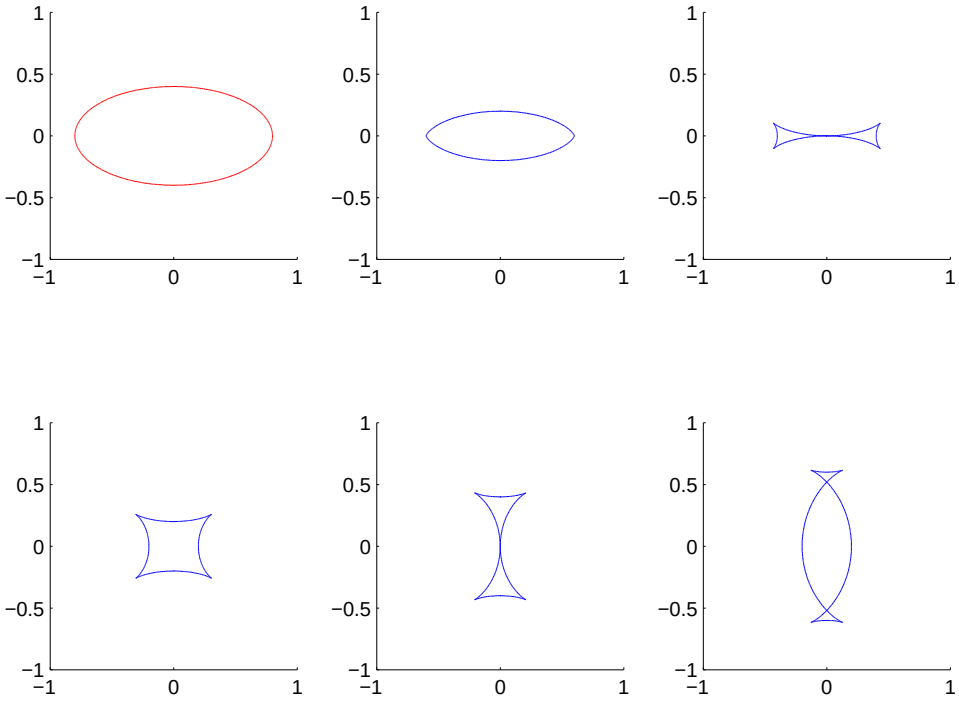

Figure 7: Wavefronts in a waveguide simulation. The index of refraction is $\eta(x, y) = 1 + e^{-y^2}$. The wavefront is initially a straight vertical line moving to the right.

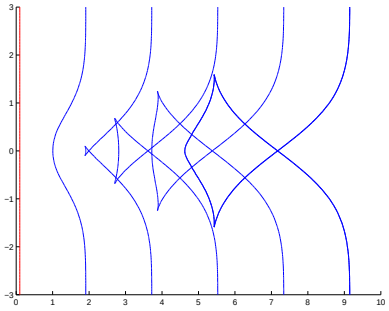

Figure 8: An example of wavefronts reflecting off the walls of the rigid boundary.

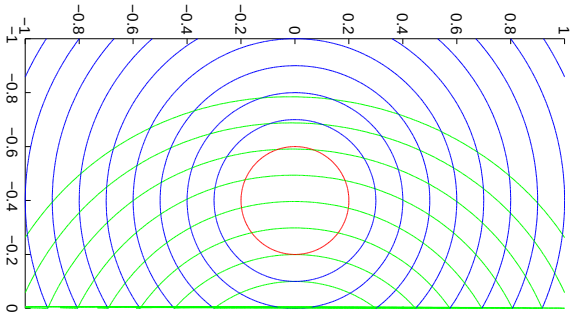

Figure 9: 3D shrinking ellipsoid.

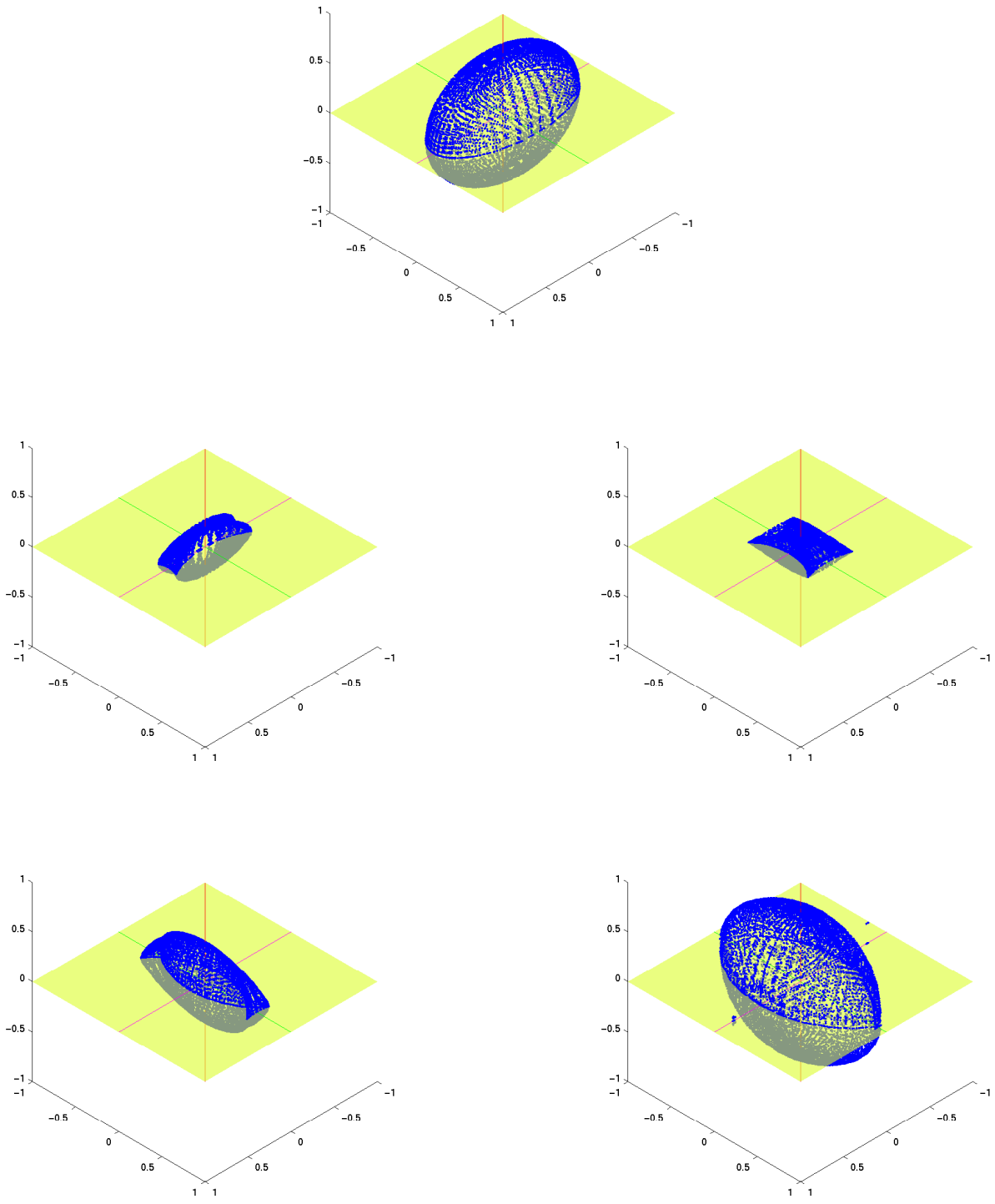

3 Visibility and the dynamics of shadows[5]

The visibility problem arises in many applications in different fields. Given a collection of three dimensional objects, we want to determine quickly the regions visible to the observer. It is a crucial step for many applications, including visualization [31] and etching [1]. For example, in a 3D virtual reality environment, knowing the visible regions helps speed up the rendering of the environment by skipping the costly computation on those occluded regions. Having an efficient visibility algorithm will prevent unnecessary computation in a large portion of the whole computational domain. Recently, there are also variational formulations for surface reconstruction that need to solve the visibility problem [36].

The majority of existing algorithms operate with objects defined by sets of polygons and use specialized hardware that has been developed for acceleration of execution speed.

The classical ideas from computational geometry community concerning ray tracing are to design data structures and algorithms that somehow classify objects in 3D according to their spatial relations so that queries about whether a ray intersects an object can be handled efficiently. The environment considered usually consists of sparse convex polygons. We refer the reader to ray tracing literatures such as [43][2] and [3].

Coorg and Teller [13][14] use a kD-tree data structure to store the polygonal occluders to exploit spatial coherence, and estimate the change in visibility in space when the viewpoint is moving (temporal coherence). The algorithm is specialized for environments with very large polygonal occluders. Though their algorithm does not handle occluder fusion, it contains some interesting ideas on selecting occluders dynamically using an "area-angle" metric

$$\frac{-A\,\vec{n}\cdot\vec{v}}{d^2},$$

where A is the area of the occluder, $\vec{n}$ its normal, x_o the viewpoint, x the point in question, and $d = |x - x_o|$, and $\vec{v} = (x - x_o)/d$.

Recently, there were two interesting papers in SIGGRAPH pertaining to visibility preprocessing for volume visualization. In [19], Durand et al found all the occluded objects by first projecting every object onto a set of reference planes. In [57], the authors consider the space discretized in rectangles/blocks using a quad/octree data structure. With opaque blocks as the interior of occluders, their algorithm then extends the opaque block along each coordinate axis according to some heuristic rules. One noticeable thing is that the authors propose to abandon considering polygons as occluders and use a volumetric approach. There are other approaches specialized for particular applications such as an urban walk-through. We refer the interested readers to the thesis of Durand [18] for an extensive overview of the literatures.

One of the simplest ideas in finding whether a point is visible to the observer is to compare the geodesic and Euclidean distances between the observer and the point of interest. However, this algorithm can only be made $\mathcal{O}(N \log N)$, where N is the number of grid points, and therefore is not optimized for real time computation. Moreover, it is subject to numerical errors.

A global visibility algorithm

We present a new level set based algorithm for finding occlusion in two and three dimensions. We are given the level set function ϕ, such that $\{\phi < 0\}$ is the interior of objects. By identifying opaque regions as the "inside" of a level set function and solving a radially defined causality relation, the algorithm gives a very accurate approximation to the occlusion with respect to a given viewing position and a set of occluders. Using a specialized occlusion sweeping, our algorithm is linear in the number of grid points surrounding the occluders and its parallelization is trivial.

[5] With P. Burchard, L.T. Cheng, S. Osher, and G. Sapiro

Occluder fusion is achieved naturally since the embedded level set function is a natural platform for merging and Boolean operations. In addition, we emphasize that our level set framework is particularly adept in handling the cases where the occluders are changing shapes continuously.

The motivation is as follows: we observe that the visibility status of points sharing the same radial direction centered at the vantage point satisfy a causality condition. Namely, if a point is occluded, then all other points further away from the vantage point in the same radial direction are also occluded. In essence, we compute the value of $\psi(x)$ by

$$\psi(x) = \min(\psi(x'), \phi(x)),$$

where x' is some point "before" x in the ray direction, depending on the grid geometry. Each grid node is visited by a specialized sweeping order that maintains the causality. Due to the minimization and the linear interpolation used to find x', the algorithm is l_∞-stable.

Multi-resolution

We can implemented the above algorithm in a multi-resolution framework. This hinges upon the ability to determine whether any given voxel is completely "inside" or "outside" of the objects.

Let C be the Lipschitz constant of ϕ. Let x_c be the center point and x_i the vertices of the given voxel V respectively. Then if

$$\phi(x_c) + C||x_c - x_i|| < 0 \ \ \forall i,$$

then we know $\phi|_V < 0$.

Dynamics of the shadow boundaries

If we are interested only in the visible faces of given objects from a moving vantage point, the most efficient algorithm would be to track the border of the visible regions. We formulate the visibility problem so that the points on the boundary of the visible regions on the surfaces can easily be identified. The dynamics of these points are derived so that one can track the visible regions according to the motion of the vantage point $x_o(t)$.

The boundaries of visible regions on given surfaces can be categorized into two:

- points that are part of the horizon/silhouette (type I);
- points that border the *shadows cast by some surface* "before" it (type II).

To every type II point x, there corresponds a type I point $x^*(x)$ such that x is the shadow of x^*; more precisely

$$x - x^*(x) \perp \nabla\phi(x^*(x)).$$

The motion of x is thus determined by that of $x^*(x)$ and the local property of $\{\phi = 0\}$.

The dynamics of the horizon

In two dimensions, we can derive the following identity from some basic geometric identities:

$$\dot{\mathbf{x}} = \begin{pmatrix} \dot{x} \\ \dot{y} \end{pmatrix} = \frac{1}{\kappa} \frac{\dot{x}_o \cdot n(\mathbf{x})}{|\mathbf{x} - \mathbf{x}_o|} n^\perp(\mathbf{x}),$$

where $n^\perp(\mathbf{x}) = (\mathbf{x} - \mathbf{x}_0)/|\mathbf{x} - \mathbf{x}_0|$. In three space dimensions, the horizon becomes a closed curve $\Gamma(s) = \mathbf{x}(s,t)$, where s is the arc length of $\Gamma(s)$.

Let P be the plane tangent to $\dot{x}_o$, passing through $\Gamma(s)$ and x_0. Let $\beta(\sigma)$ be the curve on the intersection of P and $\partial\Omega$. Then, locally at t and x, we have a two dimensional visibility problem on plane P, in which $\beta(\sigma)$

defines the boundary of the objects. Following this reasoning, κ should naturally be taken from $\beta(\sigma)$. See figure .

This can be verified by considering the two dimensional case as a section of the cylinder in 3D; i.e. the $\Omega^{(2D)}$ is really the intersection of the plane $z = 0$ and the cylinder $\Omega^{(3D)} = \Omega^{(2D)} \times \mathbb{R}$.

The dynamics of type II points

Assume that x is a type II point and x^* is its generator. In two dimensions, the motion of x is determined by the following constraints:

$$\phi(x) = 0 \text{ and } \frac{x - x^*}{|x - x^*|} = \vec{\nu}.$$

In three dimensions, we can reduce the instantaneous motion to a two dimensional problem on the "right" section of the surface.

The Shadow Generator

x and $x^*(x)$ can be related by

$$x^*(x) := x - r(x)\vec{\nu}(x), \text{ with } \vec{\nu}(x) := \frac{x - x_o}{|x - x_o|}.$$

$r(x)$ can be computed by

$$r(x) = |x - x_o| - \rho(\text{Arg}(x - x_o)),$$

where

$$\rho(\theta) = \min\{|x - x_o| : \text{Arg}(x - x_o) = \theta, \phi(x) \leq 0\}.$$

The visibility indicator

$$\Xi(x, x_o) := (x^*(x) - x) \cdot \nabla\phi(x^*(x));$$

$\{\Xi = 0\} \bigcap \{\phi = 0\}$ is the set of visible regions.

Reinitialization criterion

The visibility problem has a discontinuous nature. The invisible objects may suddenly becomes visible during the journey of the observer. With this happens, the link between type II points and their generators need to be reset. We define the inverse Gauss map $\mathcal{G}^{-1} : S^1 \mapsto \{\phi = 0\}$ such that for all $y \in \mathcal{G}^{-1}(\theta)$, $\text{Arg}(\nabla\phi(y)) = \theta$. The reinitialization is needed whenever there exist a $y \in \mathcal{G}^{-1}(\theta)$ that lies "between" x and $x^*(x)$. We can use the same multi-resolution approach mentioned above to implement this.

Figure 10: Some results of the global visibility algorithm. In the 2D cases, the occluders are represented by the green curve and the shadow boundaries

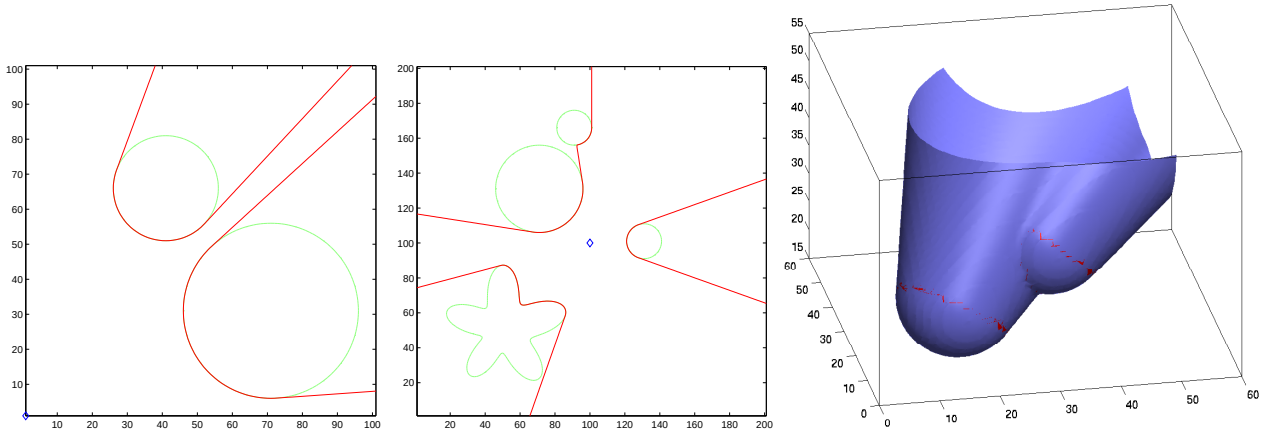

Figure 11: Reducing a 3D visibility problem to 2D by choosing the right section of the surface.

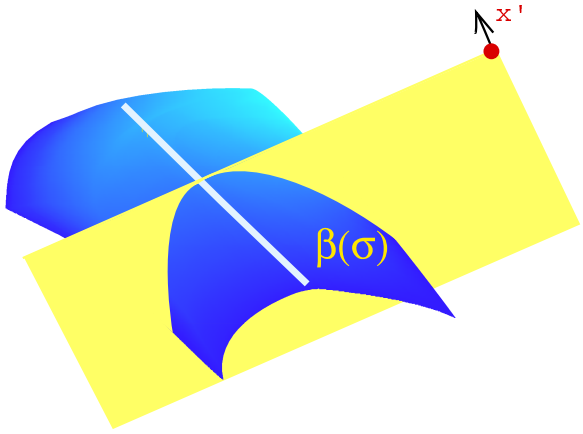

Figure 12: A 3D result. The figure on the left depicts the shadow boundary of the skeleton hand and bunny with a given vatange point. The figure on the left shows the horizon curves the generates the shadow.

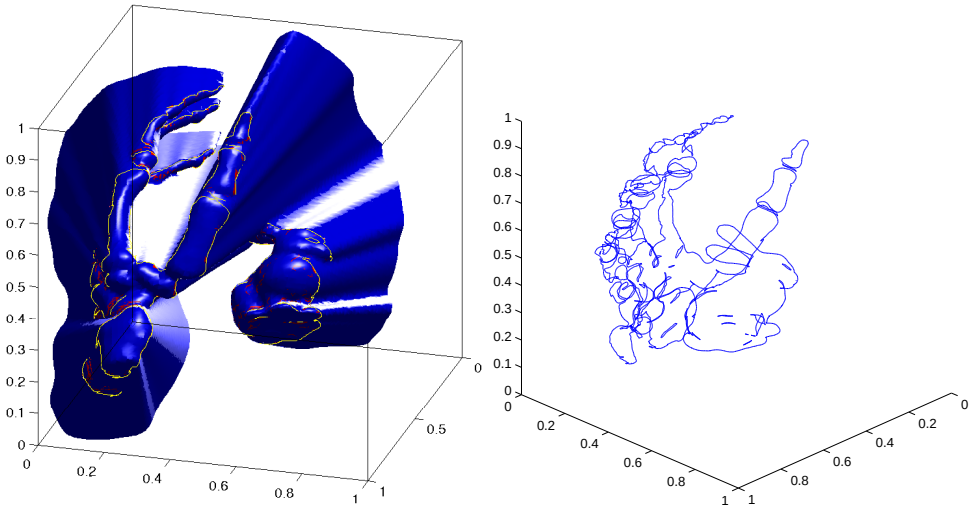

4 Fast methods for solving eikonal equations

In geometrical optics [37], the eikonal equation

$$\sqrt{\phi_x^2 + \phi_y^2} = r(x, y) \tag{8}$$

is derived from the leading term in an high frequency asymptotic expansion of the wave equation. The level sets of the solution ϕ can be interpreted as the first arrival time of the wave front that is initially Γ.

The eikonal equation also comes from control problems and its solution be interpreted as the "distance" function to Γ. We first restrict our attention to the case in which $r = 1$. Let Γ be a closed subset of $\mathbb{R}^2$. It can be shown easily that the distance function defined by

$$d(\mathbf{x}) = \text{dist}\,(\mathbf{x}, \Gamma) := \min_{p \in \Gamma} |\mathbf{x} - p|, \quad \mathbf{x} = (x, y) \in \mathbb{R}^2,$$

is the viscosity solution to equation (8) with the boundary condition

$$\phi(x, y) = 0 \ \text{ for } (x, y) \in \Gamma.$$

Rouy and Tourin [55] proved the convergence to the viscosity solution of an iterative method solving equation (8) with the Godunov Hamiltonian approximating $|\nabla \phi|$.

Osher [46] provided a link to time dependent eikonal equation by proving that the t-level set of $\phi(x, y)$ is the zero level set of the viscosity solution of the evolution equation at time t

$$\psi_t = |\nabla \psi|$$

with appropriate initial conditions. In fact, the same is true for a very general class of Hamilton-Jacobi equations (see [46]). As a consequence, one can try to solve the time-dependent equation by the level set formulation [51] with high order approximations on the partial derivatives[52][35]. Crandall and Lions proved that the discrete solution obtained with a consistent, monotone Hamiltonian converges to the desired viscosity solution [15].

Tsitsiklis [68] combined the heap sort with a variant of the classical Dijkstra algorithm to solve the steady state equation of the more general problem

$$|\nabla \phi| = r(\mathbf{x}).$$

This was later rederived in [58] and [30]. It has become known as the fast marching method whose complexity is $\mathcal{O}(N \log(N))$, where N is the number of grid points. Osher and Helmsen[49] have extended the fast marching type method to somewhat more general Hamilton-Jacobi equations.

Sweeping

Danielsson [17] proposed an algorithm to compute Euclidean distance to a subset of grid points on a two dimensional grid by visiting each grid node in some predefined orders. In [9], Boué and Dupuis suggest a similar Gauss-Seidel "sweeping" approach to solve the steady state equation which, by experience, results in a $\mathcal{O}(N)$ algorithm for the problem at hand. This "sweeping" approach has recently been used in [66] and [70] to solve for the distance functions to a class of explicitly represented Γ. Using this "sweeping" approach, the complexity of the algorithms drops from $\mathcal{O}(N \log N)$ in the fast marching to $\mathcal{O}(N)$, and the implementation of the algorithms becomes a bit easier than the fast marching method that requires heap sort.

In the following two subsections, we combine this sweeping approach to compute the "distance" function under different settings.

4.1 Computing the distance function to a class of explicitly defined interfaces[6]

Motivation of algorithms

The motivation for the algorithms comes from considering Huygens' principle "backwards" . Let E be the point on which we want to find the distance value. Huygens' principle can be viewed as sending circular waves from each point in the neighborhood of E at times prescribed by the distance function, and asking for the envelope of the waves at a certain time.

We restrict ourselves to two dimensions for simplicity of exposition. Let us first consider a single generator; i.e. $\Gamma = \{\gamma_0 \in \Omega\}$, whose location is unknown. Suppose r_1 and r_2 are the distance of two distinct points $P = (x_1, y_1)$, $Q = (x_2, y_2)$ to Γ, respectively: i.e. $u(P) = r_1, u(Q) = r_2$. Let $E = (x, y)$ be a point of interest with

$$|E - \gamma_0| \geq \max\{u(P), u(Q)\}. \tag{9}$$

Draw a circle C_P of radius r_1 centered at P and a circle C_Q of radius r_2 centered at Q. It is then easy to see that C_P and C_Q intersect, and one of the intersections is γ_0. Since the equations are quadratic, there might be two intersections, W and V. From the hypothesis that E is farther from γ_0 than P and Q, we know that $u(E) = \max\{|E - W|, |E - V|\}$.

Thus, by enforcing this sort of ***upwinding decision*** when selecting intersections, we are able to approximate the distance function. In fact, this is the key property for the success of the aforementioned fast marching and sweeping methods.

Generalization

In the spirit of Steinhoff's Dynamic Surface Extension [63], we can define functions that map each point in $\mathbb{R}^3$ to the space of (local) representations of surfaces (heretherto referred as surface elements). We can further define the distance of a point P and a surface element $\mathcal{S}$

$$\text{dist}(P, \mathcal{S}) := \min_{y \in S}(P, y).$$

The 'surface element' can be for example the tangent plane, the curvature, or a NURB description of the surface.

In stead of propagating distance values away from the interface, *we propagate the surface element information along the characteristics* and impose conditions that e*nforce the first arrival property* of the viscosity solution of eikonal equation. The challenge is to compute the exact distance from a given surface element and to derive the "upwinding" criteria for propagating the surface information throughout the grids.

Given a smooth parametrized surface $\Sigma : I_s \times I_t \mapsto \mathbb{R}^3$, our algorithm provides accurate initial guess for Newton's iterations on the orthogonality identity. The initial guess in this case is simply the closest points of the neighbors of $\mathbf{x}$.

Figures 13, 14, and 15 show our results for some examples.

4.2 Fast methods for anisotropic eikonal equation[7]

The problem of finding the distance function in anisotropic medium can be modeled by a slightly more general form of Hamilton-Jacobi equation:

$$\sqrt{a\phi_x^2 + b\phi_y^2 - 2c\phi_x\phi_y} = r(x, y), \quad a, b > 0, ab > c^2. \tag{10}$$

[6] To appear in J. Comput. Phys.

[7] With L.T. Cheng, S. Osher, and H.K. Zhao, submitted to SIAM J. Num. Anal.

Figure 13: Comparison between Godunov solution (left) and our algorithm (right). The isosurface of the distance function to a set of isolated points is plotted.

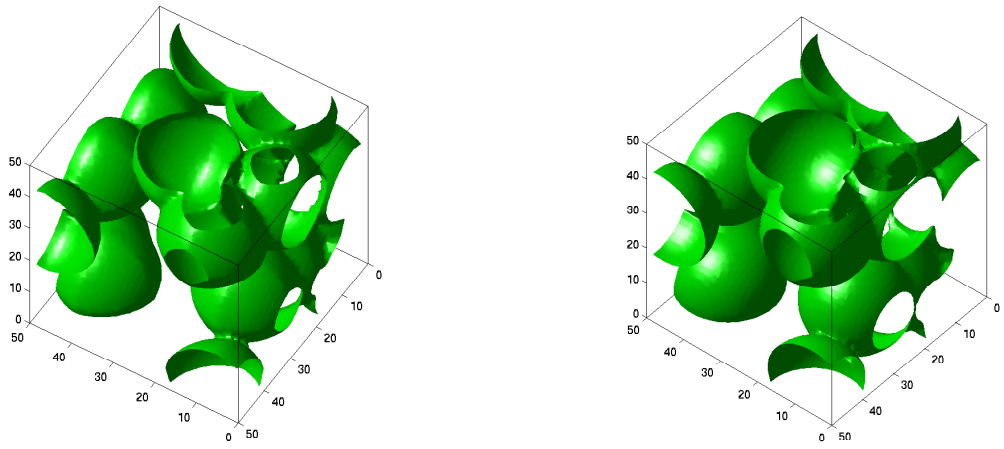

Figure 14: Two 2 dimensional examples. Distance contours to Γ are plotted.

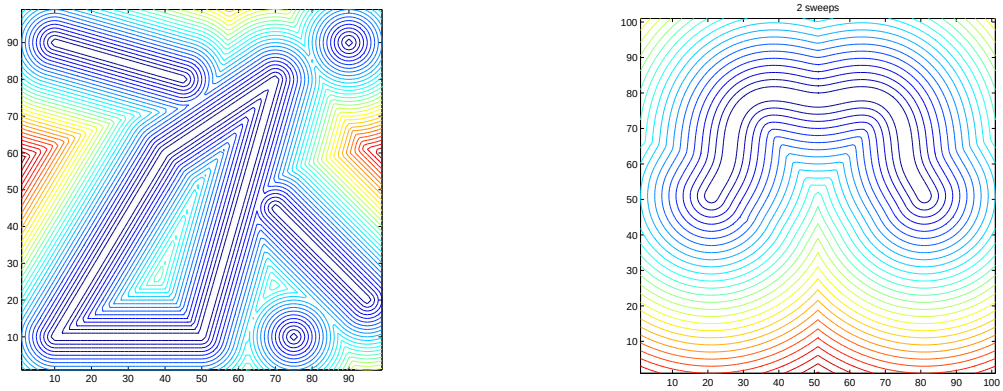

Figure 15: 3D examples. Here we show the isosurfaces of some given objects.

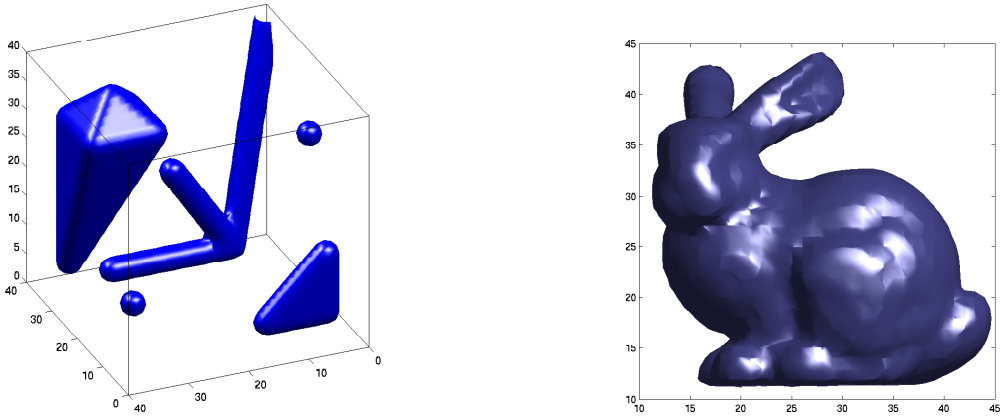

This occurs in many applications; e.g. ray tracing in crystals. Another example is the geodesic distance function on the graph of a smooth function $f(x, y)$. It can be shown [67] that the geodesic distance satisfies

$$(1 - \frac{f_x^2}{f_x^2 + f_y^2 + 1})\phi_x^2 + (1 - \frac{f_y^2}{f_x^2 + f_y^2 + 1})\phi_y^2 - 2\frac{f_x f_y}{f_x^2 + f_y^2 + 1}\phi_x\phi_y = 1 \tag{11}$$

At this point, one might ask if fast marching method can be used to construct approximate solutions to this class of HJ equations? For a given Hamiltonian $H(p, q)$, regardless of its convexity, Osher's fast marching criterion

$$pH_p \geq 0, qH_q \geq 0 \tag{12}$$

ensures the applicability of the fast marching heap sort strategy. In the class of Hamiltonians that we consider

$$H(p, q) = \sqrt{ap^2 + bq^2 - 2cpq},$$

as long as $c \neq 0$, it is likely that the above criterion is not satisfied.

Instead, we use the Gauss-Seidel (sweeping) strategy to update the grid values. To compute approximations that converges to the viscosity solution, we solve the value of each grid node in terms of its four neighbors according to the quadratic equation formed by the monotone upwinding Godunov Hamiltonian [4] and the forcing function r:

$$H_G(p_+, p_-; q_+, q_-) = \text{ext}_{p \in I[p_-, p_+]}\text{ext}_{q \in I[q_-, q_+]}H(p, q) = r. \tag{13}$$

In [67], we derive an explicit expression of the Godunov Hamiltonian in the form:

$$H_G(p, q_-, q_+) = H(p, \text{sgn}\max\{(q_- - q_\sigma)^+, (q_+ - q_\sigma)^-\} + q_\sigma), \tag{14}$$

where

$$\begin{aligned} \text{sgn}\max(x, y) &= \quad x^+ \quad \text{if} \quad \max\{x^+, y^-\} = x^+ \\ \text{sgn}\max(x, y) &= -y^- \quad \text{if} \quad \max\{x^+, y^-\} = y^-, \end{aligned}$$

and a straight forward algorithm to solve the resulting quadratic equations.

Comparisons to the steady state viscosity solution of

$$\tilde{\phi}_t + \text{sgn}(\phi(x, y))(H(x, y, \tilde{\phi}_x, \tilde{\phi}_y) - r(x, y)) = 0. \tag{15}$$

where $\tilde{\phi}(x, y, t = 0) = \phi(x, y) = 0$ for $(x, y) \in \Gamma$, and ϕ is the solution obtained from the sweeping algorithm, and to the case with known geodesic distance, suggest that our approximations converge to the right viscosity solution numerically. Figure 16 and 17 shows the contours of the geodesic distance functions in different settings.

Figure 16: Examples of constant coefficients case with oscillatory forcing $r(x) = 2.1 - \cos(4\pi^2 xy)$. Left: $a = 1$, $b = 1$, $c = 0$, on a 200x200 grid, convergence is reached in 7 sweeping iterations. Right: (A very degenerate case) $a = 0.375$, $b = 0.25$, $c = 0.29$. , on a 100x100 grid. Notice that in this case, $ab = 0.0938$ is barely greater than $c^2 = 0.0841$. The contour of the solution is plotted. The convergence is reached at 43 sweeping iterations.

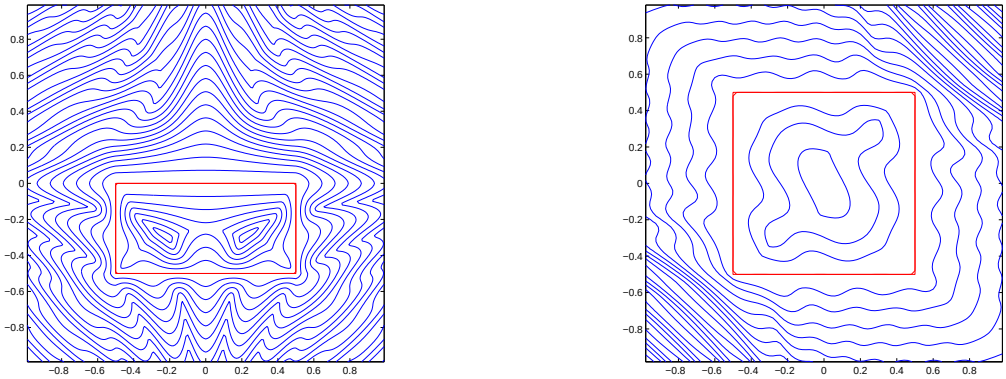

Figure 17: Examples of distance function on graphs. Left: $f(x, y) = \sqrt{1.0 - (x^2 + y^2)}$, The convergence is reached after 2 sweeping iterations on a 100x100 grid. Right: $f(x, y) = \cos(2\pi x)\sin(2\pi y)$, convergence after 9 iterations on a 100x100 grid.

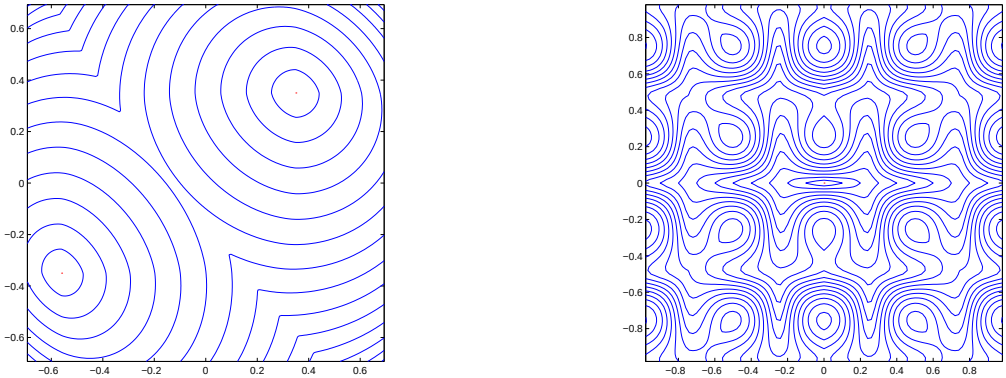

5 A look at the future

Each of the topics mentioned above provides further research directions. I will first put down a brief listing of the problems that I am working on or interested in, and elaborate on those in which I have some preliminary results.

- Phase-space level set methods [47]
  - geometrical optics
  - fast marching implementation
  - the motion of open curves and spiral crystal growth in materials science
- Motion by mean curvature of data sets in high dimension
- Strong Vertical Diffusion [65]
  - bunching effects in crystal growth(in preparation)
  - systems of conservation laws
  - applications to optimal control problems
- Visibility
- Image Processing: affine total variation image restoration, shape from shading, and morphing
- Supra-convergence on irregular grids

5.1 Supra-convergence of some numerical schemes on irregular grids[8]

In addition to the topics described in the previous sections, I have also worked on the convergence properties of a class of finite difference scheme of linear time dependent PDEs on irregular grids.

Numerical experiments suggest a second order accuracy of the Numerov scheme for the first and second order wave equations in 1 dimension with suitable regularizing terms. Following the paper of Kreiss and Manteuffel on supra-convergence [40], we explore the special summing structure and prove second order accuracy for linear heat equations.

5.2 Visibility

We have endeavored to look at the visibility problem of a moving vantage point. Our next step will be to fully use the strength of the level set methods in handling topological changes to study the visibility problem of morphing or pulsating objects.

The visibility problem is a complex one in the sense that: 1) there are discontinuities in space and time 2) there are mathematical considerations on the formulation and the solution of the problem as well as the computer science type data structure considerations. In light of 1), I am trying to apply the state of the art shock calculation methods and theories to the visibility problem.

5.3 Strong vertical diffusion

From the discussion of the singular diffusion term above, we see intuitively the similarity of the convexification of the speed function over the jumps to the Lax-Oleinik formula [41] and Osher's formula [44, 45] for the solution to the Riemann problem. We are currently investigating this link.

[8] With H-O Kreiss and L.T. Cheng, in preparation.

Figure 18: Example of anisotropic curvature motion and bunching

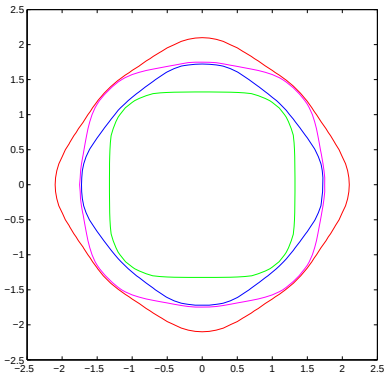

5.3.1 Anisotropic curvature motion and bunching

In [50, 54] the authors studied the problem of Wulff shapes that is related to the single sheet crystal growth by Hamilton-Jacobi equations. See also [60]. It is observed in experiments [69] that actual crystal growth consist of different sheets, each with the same Wulff shape in different orientation. In addition, viewing from the side, the height of the sheets structure remains as graph of a function. The formation of jump discontinuities in height is called bunching.

We study anisotropic bunching in crystal growth [26][39] under curvature and a singular vertical diffusive regularization: $u : \mathbb{R}^n \times \mathbb{R}^+ \mapsto \mathbb{R}$,

$$u_t + M(u, \nabla u)(\nabla \cdot \frac{\nabla u}{|\nabla u|} + C)|\nabla u| = 0.$$

The function $M : \mathbb{R} \times \mathbb{R}^n \mapsto \mathbb{R}$ is usually called the mobility function, which determines the anisotropic motion of the crystal. If M is increasing in u, then shock may develop even if the initial data is smooth. Following [65], we propose a level set formulation with a singular vertical diffusion regularization:

$$\phi_t + M(x_{n+1}, \nabla_{x_1,\cdots,x_n}\phi)(\nabla_{x_1,\cdots,x_n} \cdot \frac{\nabla_{x_1,\cdots,x_n}\phi}{|\nabla_{x_1,\cdots,x_n}\phi|} + C)|\nabla_{x_1,\cdots,x_n}\phi| = \eta|\nabla_{\mathbb{R}^{n+1}}\phi|\frac{\partial}{\partial x_{n+1}}\frac{\phi_{x_{n+1}}}{|\phi_{x_{n+1}}|}.$$

See figure 18 for an preliminary result. It is a superposition of different level sets corresponding to the Wulff shapes in each sheet. Our singular diffusion term successfully prevents level sets from "over-turning" and the curvature term seems to keep the convexity of the shapes.

5.3.2 Systems of conservation laws

We are generalizing the result of our singular viscosity to study the solution of conservation laws system and the link to Riemann invariants. Here we briefly describe how we are approaching this problem.

Let $\vec{u} = (u, v) \in \mathbb{R}^2$, $\phi(t, x, y) : \mathbb{R}^+ \times \mathbb{R} \times \mathbb{R}^2 \mapsto \mathbb{R}^2$ be the vector values level set function such that $\phi(t, x, \vec{u}(t, x)) = 0$. The system

$$\vec{u}_t + A(\vec{u})\vec{u}_x = 0$$

can be formally translated to

$$\phi_t + \phi_y A(y)\phi_y^{-1}\phi_x = 0.$$

We shall use the Riemann invariants for the 2×2 system to diagonalize $A(y)$ and desingularize the term ϕ_y^{-1}.

We propose a singular diffusion term similar to the scalar one we used. With an abuse of notation, this term can be written as

$$|\nabla_{x,y}\phi|\nabla_y \cdot (|\nabla_y \phi|^{-1}\nabla_y \phi),$$

where $\nabla_{x,y}\phi$ is the Jacobian matrix of ϕ with respect to x and y, $\nabla_y \phi = \phi_y$ is the Jacobian matrix of ϕ, and $|A| := \sqrt{AA^*}$ is the Euclidean norm of the matrix A.

5.4 Phase-space level set method

By characterizing an open curve using the phase space level set method [47], we do not have the difficulties commonly encountered by level set methods. I would like to further study the motion of open curves in different fields.

5.4.1 Spiral crystal growth

In epitaxial growth of high-temperature superconducting thin films, the spirals are generally believed to be a step that terminates at a screw dislocation. As atoms attach to the step, it moves normal to itself except at the dislocation, thus resulting in spiral form. This was first theorized by Burton, Cabrera and Frank in [11]. There have been other theoretical investigations in the spiral motion as well as the numerical implementations. Please see [59] and [69] for more detail.

I would like to use the phase space level set method to study this topic. An ultimate goal is to unify the spiral crystal growth and the bunching phenomenon using the singular diffusion term, and thus provide a mathematical theory and computational framework for simulation.

References

[1] D. Adalsteinsson and J.A. Sethian. An overview of level set methods for etching, deposition, and lithography development. *IEEE Transactions on Semiconductor Devices*, 10(1), February 1997.

[2] Pankaj K. Agarwal and Micha Sharir. Ray shooting amidst convex polygons in 2D. *J. Algorithms*, 21(3):508–519, 1996.

[3] Pankaj K. Agarwal and Micha Sharir. Ray shooting amidst convex polyhedra and polyhedral terrains in three dimensions. *SIAM J. Comput.*, 25(1):100–116, 1996.

[4] Martino Bardi and Stanley Osher. The nonconvex multi-dimentional Riemann problem for Hamilton-Jacobi equations. *SIAM J Math Anal*, 22(2):344–351, 1991.

[5] Guy Barles. Discontinuous viscosity solutions of first-order Hamilton-Jacobi equations: a guided visit. *Nonlinear Anal.*, 20(9):1123–1134, 1993.

[6] E. N. Barron and R. Jensen. Semicontinuous viscosity solutions for Hamilton-Jacobi equations with convex Hamiltonians. *Comm. Partial Differential Equations*, 15(12):1713–1742, 1990.

[7] Jean-David Benamou. Direct computation of multivalued phase space solutions for Hamilton-Jacobi equations. *Comm. Pure Appl. Math.*, 52(11):1443–1475, 1999.

[8] Jean-David Benamou and Ian Solliec. An Eulerian method for capturing caustics. *J. Comput. Phys.*, 162(1):132–163, 2000.

[9] Michelle Boué and Paul Dupuis. Markov chain approximations for deterministic control problems with affine dynamics and quadratic cost in the control. *SIAM J Num Anal*, 1998.

[10] Paul Burchard, Li-Tien Cheng, Barry Merriman, and Stanley Osher. Motion of curves in three spatial dimensions using a level set approach. *UCLA CAM Report*, 00(29), 2000. To appear, Journal of Computational Physics (2001).

[11] W. K. Burton, N. Cabrera, and F. C. Frank. The growth of crystals and the equilibrium structure of their surfaces. *Philos. Trans. Roy. Soc. London. Ser. A.*, 243:299–358, 1951.

[12] Li-Tien Cheng, Paul Burchard, Barry Merriman, and Stanley Osher. Motion of curves constrained on surfaces using a level set approach. *UCLA CAM Report*, 00(32), 2000. To appear, Journal of Computational Physics (2001).

[13] Satyan Coorg and Seth Teller. Real-time occlusion culling for models with large occluders. In *ACM Symposium on Interactive 3D Graphics*, 1997.

[14] Satyan Coorg and Seth Teller. Temporally coherent conservative visibility. *Comput. Geom.*, 12(1-2):105–124, 1999. 12th ACM Symposium on Computational Geometry (Philadelphia, PA, 1996).

[15] M.G. Crandall and P.L. Lions. Two approximations of solutions of Hamilton-Jacobi equations. *Mathematics of Computation*, 43:1–19, 1984.

[16] Michael G. Crandall and Pierre-Louis Lions. Viscosity solutions of Hamilton-Jacobi equations. *Trans. Amer. Math. Soc.*, 277(1):1–42, 1983.

[17] Per-Erik Danielsson. Euclidean distance mapping. *Computer Graphics and Image Processing*, 14:227–248, 1980.

[18] Fredo Durand. 3d visibility: Analysis study and applications. *PhD Thesis, MIT*, 1999.

[19] Fredo Durand, George Drettakis, Joëlle Thollot, and Claude Puech. Conservative visibility preprocessing using extended projections. In *SIGGRAPH*, 2000.

[20] Björn Engquist and Olof Runborg. Multiphase computations in geometrical optics. In *Hyperbolic problems: theory, numerics, applications, Vol. I (Zürich, 1998)*, pages 273–284. Birkhäuser, Basel, 1999.

[21] Björn Enquist, Olof Runbord, and Anna-Karin Tornberg. High frequency wave propagation by the segment projection method. *UCLA CAM Report*, 01(13), 2001.

[22] Lawrence C. Evans. A geometric interpretation of the heat equation with multivalued initial data. *SIAM J. Math. Anal.*, 27(4):932–958, 1996.

[23] Mi-Ho Giga and Yoshikazu Giga. Crystalline and level set flow—convergence of a crystalline algorithm for a general anisotropic curvature flow in the plane. In *Free boundary problems: theory and applications, I (Chiba, 1999)*, pages 64–79. Gakkōtosho, Tokyo, 2000.

[24] Mi-Ho Giga, Yoshikazu Giga, and Ryo Kobayashi. Very singular diffusion equations. In *Advanced Studies in Pure Mathematics 31, 2001*, pages 93–125, 2001.

[25] Y. Giga, S. Goto, H. Ishii, and M.-H. Sato. Comparison principle and convexity preserving properties for singular degenerate parabolic equations on unbounded domains. *Indiana Univ. Math. J.*, 40(2):443–470, 1991.

[26] Yoshikazu Giga. Moving boundary equations with anisotropic curvature. *Sūgaku*, 52(2):113–127, 2000.

[27] Yoshikazu Giga. Shocks and very strong vertical diffusion. In *To appear, Proc. of international conference on partial differential equations in celebration of the seventy fifth birthday of Professor Louis Nirenberg, Taiwan*, 2001.

[28] Yoshikazu Giga. Viscosity solutions with shocks. *Hokkaido Univ. Preprint Series in Math.*, (519), 2001.

[29] Yoshikazu Giga and Moto-Hiko Sato. A level set approach to semicontinuous viscosity solutions for Cauchy problems. *Comm. Partial Differential Equations*, 26(5-6):813–839, 2001.

[30] J. Helmsen, E. Puckett, P. Colella, and M. Dorr. Two new methods for simulating photolithography development in 3d. In *SPIE 2726*, pages 253–261, 1996.

[31] Aaron Hertzmann and Denis Zorin. Illustrating smooth surfaces. In *SIGGRAPH*, 2001.

[32] Hitoshi Ishii. Hamilton-Jacobi equations with discontinuous Hamiltonians on arbitrary open sets. *Bull. Fac. Sci. Engrg. Chuo Univ.*, 28:33–77, 1985.

[33] Hitoshi Ishii. Existence and uniqueness of solutions of Hamilton-Jacobi equations. *Funkcial. Ekvac.*, 29(2):167–188, 1986.

[34] Hitoshi Ishii. Perron's method for Hamilton-Jacobi equations. *Duke Math. J.*, 55(2):369–384, 1987.

[35] Guang-Shan Jiang and Danping Peng. Weighted ENO schemes for Hamilton-Jacobi equations. *SIAM J. Sci. Comput.*, 21(6):2126–2143 (electronic), 2000.

[36] Hailin Jin, Anthony Yezzi, and Stefano Soatto. Stereoscopic shading: Integating multi-frame shape cues in a variational framework. *In Preparation*.

[37] Joseph B. Keller. Geometrical theory of diffraction. *J. Opt. Soc. Amer.*, 52:116–130, 1962.

[38] R. Kobayashi and Y. Giga. Equations with singular diffusivity. *J. Statist. Phys.*, 95(5-6):1187–1220, 1999.

[39] Ryo Kobayashi and Yoshikazu Giga. On anisotropy and curvature effects for growing crystals. *Japan J. Indust. Appl. Math.*, 18(2):207–230, 2001. Recent topics in mathematics moving toward science and engineering.

[40] H-O Kreiss, T.A. Manteuffel, B. Swartz, B. Wendroff, and A.B. White Jr. Supra-convergence schemes on irregular grids. *Mathematics of Computation*, 47:537–554, 1986.

[41] Peter D. Lax. *Hyperbolic systems of conservation laws and the mathematical theory of shock waves*. Society for Industrial and Applied Mathematics, Philadelphia, Pa., 1973. Conference Board of the Mathematical Sciences Regional Conference Series in Applied Mathematics, No. 11.

[42] Chi-Tien Lin and Eitan Tadmor. High-resolution nonoscillatory central schemes for Hamilton-Jacobi equations. *SIAM J. Sci. Comput.*, 21(6):2163–2186 (electronic), 2000.

[43] Shai Mohaban and Micha Sharir. Ray shooting amidst spheres in three dimensions and related problems. *SIAM J. Comput.*, 26(3):654–674, 1997.

[44] Stanley Osher. The Riemann problem for nonconvex scalar conservation laws and Hamilton-Jacobi equations. *Proc. Amer. Math. Soc.*, 89(4):641–646, 1983.

[45] Stanley Osher. Riemann solvers, the entropy condition, and difference approximations. *SIAM J. Numer. Anal.*, 21(2):217–235, 1984.

[46] Stanley Osher. A level set formulation for the solution of the Dirichlet problem for Hamilton-Jacobi equations. *SIAM J Math Anal*, 24(5):1145–1152, 1993.

[47] Stanley Osher, Li-Tien Cheng, Myungjoo Kang, Hyeseon Shim, and Yen-Hsi Tsai. Geometric optics in a phase space based level set and eulerian framework. 2001. Submitted to Journal of Computational Physics.

[48] Stanley Osher and Ronald P. Fedkiw. Level set methods: an overview and some recent results. *J. Comput. Phys.*, 169(2):463–502, 2001.

[49] Stanley Osher and J. Helmsen. A generalized fast algorithm with applications to ion etching. *In Preparation.*

[50] Stanley Osher and Barry Merriman. The Wulff shape as the asymptotic limit of a growing crystalline interface. *Asian J. Math.*, 1(3):560–571, 1997.

[51] Stanley Osher and James A. Sethian. Fronts propagating with curvature-dependent speed: algorithms based on Hamilton-Jacobi formulations. *J. Comput. Phys.*, 79(1):12–49, 1988.

[52] Stanley Osher and Chi-Wang Shu. High-order essentially nonoscillatory schemes for Hamilton-Jacobi equations. *SIAM J. Numer. Anal.*, 28(4):907–922, 1991.

[53] Danping Peng, Barry Merriman, Stanley Osher, Hongkai Zhao, and Myungjoo Kang. A PDE-based fast local level set method. *J. Comput. Phys.*, 155(2):410–438, 1999.

[54] Danping Peng, Stanley Osher, Barry Merriman, and Hong-Kai Zhao. The geometry of Wulff crystal shapes and its relations with Riemann problems. In *Nonlinear partial differential equations (Evanston, IL, 1998)*, pages 251–303. Amer. Math. Soc., Providence, RI, 1999.

[55] Elisabeth Rouy and Agnés Tourin. A viscosity solutions approach to shape-from-shading. *SIAM J Num Anal*, 29(3):867–884, 1992.

[56] Steven J. Ruuth, Barry Merriman, and Stanley Osher. A fixed grid method for capturing the motion of self-intersecting interfaces and related pdes. *Journal of Computational Physics*, 163:1–21, 2000.

[57] Gernot Schaufler, Julie Dorsey, Xavier Decoret, and Francois X. Sillion. Conservative volumetric visibility with occluder fusion. In *SIGGRAPH*, 2000.

[58] J.A. Sethian. Fast marching level set methods for three dimensional photolithography development. In *SPIE 2726*, pages 261–272, 1996.

[59] Peter Smereka. Spiral crystal growth. *Phys. D*, 138(3-4):282–301, 2000.

[60] Pierpaolo Soravia. Generalized motion of a front propagating along its normal direction: a differential games approach. *Nonlinear Anal.*, 22(10):1247–1262, 1994.

[61] Panagiotis E. Souganidis. Approximation schemes for viscosity solutions of Hamilton-Jacobi equations. *J. Differential Equations*, 59(1):1–43, 1985.

[62] R.J. Spiteri and S.J. Ruuth. A new class of optimal high-order strong-stability-preserving time discretization methods. Preprint).

[63] J Steinhoff and M Fan. Eulerian computation of evolving surfaces, curves and discontinuous fields. *Technical Report, University of Tennessee Space Institute*, (37388), 1998.

[64] A.-K. Tornberg and B. Engquist. Interface tracking in multiphase flows. In *Multifield problems*, pages 58–65. Springer, Berlin, 2000.

[65] Yen-Hsi Tsai, Yoshikazu Giga, and Stanley Osher. A level set approach for computing discontinuous solutions of a class of hamilton-jacobi equations. *UCLA CAM Report* , 01(05), 2001. To appear, Mathematics of Computations.

[66] Yen-Hsi Richard Tsai. Rapid and accurate computation of the distance function using grids. *UCLA CAM Report* , 00(36), 2000. To appear, Journal of Computational Physics (2001).

[67] Yen-Hsi Richard Tsai, Li-Tien Cheng, Stanley Osher, and Hong-Kai Zhao. Fast sweeping methods for a class of hamilton-jacobi equations. *UCLA CAM Report* , 01(27), 2001.

[68] John Tsitsiklis. Efficient algorithms for globally optimal trajectories. *IEEE Transactions on Automatic Control*, 40(9):1528–1538, 1995.

[69] William R. Wilcox. *Preparation and Properties of Solid State Materials*, volume 7.

[70] Hong-Kai Zhao, Stanley Osher, Barry Merriman, and Myungjoo Kang. Implicit and non-parametric shape reconstruction from unorganized points using variational level set method. *Computer Vision and Image Understanding*, 80:295–319, 2000.